Modeling the Links Between the Chemical, Electrical and Contractile Calcium Dynamics in a Heart Cell

REU Site: Interdisciplinary Program in High Performance Computing

Kallista Angeloff[1], Carlos Barajas[2], Alexander Middleton[3], Uchenna Osia[4]
Graduate assistant: Jonathan S. Graf[5], Faculty mentor: Matthias K. Gobbert[5], and
Client: Zana Coulibaly[6]

[1]Department of Atmospheric Sciences, University of Washington,
[2]Department of Mathematics and Computer Science, Olivet College,
[3]Department of Mathematics, Winthrop University,
[4]Department of Computer Science and Electrical Engineering, UMBC,
[5]Department of Mathematics and Statistics, UMBC,
[6]Department of Pharmacology, University of California, Davis

Technical Report HPCF–2016–15, hpcf.umbc.edu > Publications

Abstract

Calcium dysregulation is a significant cause of fatal cardiac arrythmias, but it is an incompletely understood phenomenon and difficult to predict. Cardiac calcium levels can be modelled as a system of partial differential equations linking the electrical, calcium, and mechanical dynamics of the heart. Earlier work on this subject established a model linking the chemical and electrical systems, which did not include the contractile or mechanical influence. We have expanded the most recent extant model to include the mechanical aspect of calcium dynamics in the heart.

Key words: Calcium-induced calcium release, Cardiomyocytes, Contractile cardiac dynamics, Chemical cardiac dynamics, Electrical cardiac dynamics

1 Introduction

Heart disease is currently the leading cause of death in the United States, according to the Center for Disease Control and Prevention. Calcium dysregulation is a signicant cause of fatal cardiac arrhythmia, but it is an incompletely understood phenomenon [1]. The current treatment for cardiac arrhythmia, mild or otherwise, is surgical implantation of a pacemaker to artificially stimulate the electrical patterns which would beregulated by calcium levels in a healthy heart. To date, no medication has been developed that been proven to be effective in in more than a handful cases [1].

Though devices like pacemakers have proven to help reduce the death rate due to arrythrmia they do not prevent onset arrythmia. It is probable that a more indepth understanding of the the ionized calcium, Ca^{2+}, might yield new methods in the realm of drug therapy. In order to better study the heart examining individual cells and three components associated with them: electrical excitation, calcium signaling, and mechanical contraction. These three systems are coupled together as seen in Figure 1.1 with calcium signaling being the central dynamic between the top system, electrical excitation, and the bottom system, mechanical contraction.

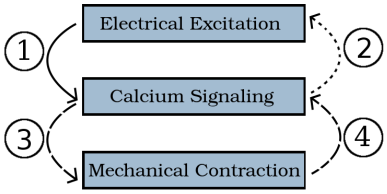

Figure 1.1: The calcium-mediated contractile rhythm of a given cardiomyocyte is a function of three coupled dynamics: electrical excitation, calcium signaling, and mechanical contraction.

The couplings that are shown in Figure 1.1 each represent a biological process inside the cardiac cell. The calcium inside the heart cell is contained inside of the sarcoplasmic reticulum (SR). The SR has calcium sensitive sites called calcium release units (CRU) which, when the concentration of calcium is high enough, release calcium into the cytosol of the cell. Calcium can enter the cytosol of the cell through an L-type calcium channel (LCC) when the cell membrane becomes depolarized. The depolarization of the cell memebrane occurs when calcium is pumped out of the cell and sodium is pumped into the cell through the sodium calcium exchanger. While these systems processess are interacting, calcium is also binding and unbinding to immobile contractile proteins inside of the cytosol. The contractile proteins are attached to musclular strands known as sacromere and the cell expands and contracts based on the amount of calcium bound in this fashion. A closer analysis of these interactions is present inside Section 2.

We represent the electrical excitation, calcium signaling, and mechanical contraction which control the contractile rhythm of an individual cardiomyocyte by a system of eight time-dependent coupled PDEs. The calcium signaling is described by five PDEs modelling concentrations of calcium ions and buffer species in the cytosol and SR. The electrical excitation is represented by two PDEs, one representing voltage and one representing the concentration of an additional electrolyte, potassium. The mechanical contraction is described by a final PDE representing the concentration of actively linked contractile proteins in the cytosol. The exact definitions of the partial differential equations can be found in Section 3.

There is a system of time dependent parabolic partial differential equations used to model our problem. These PDEs are coupled between the three systems. The domain shape, a rectangular prism is modeled after the brick shape of a heart cell. We use a method of lines (MOL) approach to spatially discretize this model and finite volume method (FVM) for spatial discretization. The implementation of this is done in C using MPI commands. A more exhuastive overview can be found in Section 4.

In Section 5, we present numerical simulations of our model to examine the behavior of different solutions. We consider both one- and two-way coupling between the electrical and calcium signaling systems. For two-way coupling, we present a parameter study to examine how our solutions are impacted.

2 Background

The general structure of cardiomyocytes on the heart can be seen in Figure 2.1(a) just below.

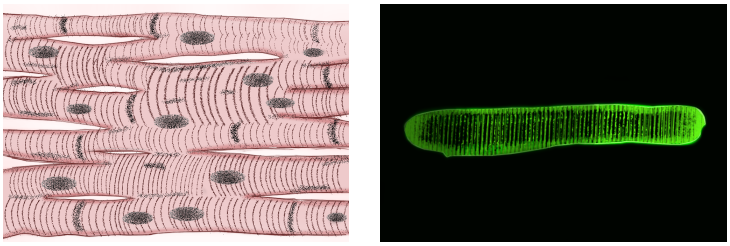

(a) Cardiac cell structure (b) Calcium filled cardiomyocyte

Figure 2.1: (a) A conglomerate of cardiac cells. The muscle fibers of each heart cell contract in response to the change in shape of contractile proteins, in turn mediated by calcium levels in the cytosol. These muscle fibers can be seen as darker striations throughout the cell. (b) An individual heart cell illuminated by fluoro-4, a fluorescent dye, undergoing a calcium wave.

The general shape of the cardiac cell is rectangular with several T-tubules along the side of the cell. The light pink areas of Figure 2.1(a) represent the cellular membrane of the cardiomyocyte. The muscle fibers run parallel to the contractile proteins of the cardiac cell. The dark splotches are the cell nuclei associated with their respective cell. Inside the cardiomyocyte is the sacroplasmic reticulum (SR), a type of container, contains both calcium ions and calsequestrian (CQ). The release of calcium from the SR into the cytosol occurs via calcium release units (CRUs) on the SR. Once the concentration is high enough the CRUs will begin to open also called sparking; sparking is the scattered, local simultaneous opening of a small number of CRUs. The fluorescent dye is mixed in the cytosol and used to make the calcium more visible during lab experiments; the dye diffuses through the cytosol interacting with and binding to calcium in the cytosol. How these components combine to affect small strands of muscle fiber and cause cell pulsation is shown in Figure 2.2.

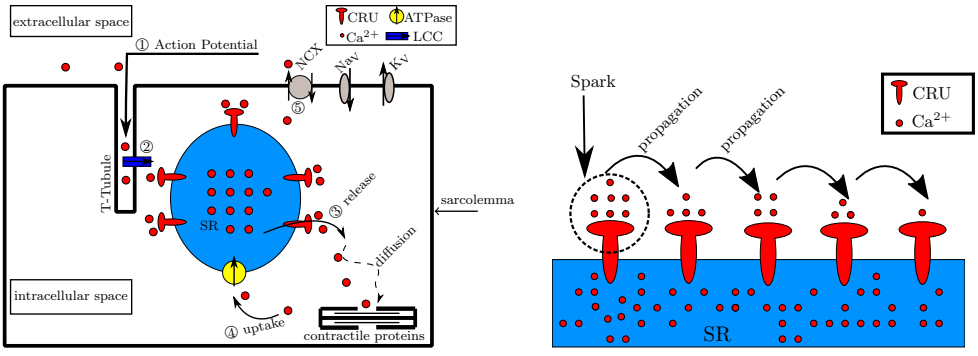

(a) CICR (b) Sparking Behavior

Figure 2.2: (a) The T-tubules enfold the L-type calcium channels (LCC) in the cell's plasma membrane. Periodic membrane depolarizations allow calcium to pass into the cytosol. (b) Calcium released from the calcium release units (CRUs) on the SR and begin the cascading calcium release that starts calcium wave propagation.

The sodium-calcium electrical exchange pushes a calcium ion out of the cell while bringing three sodium ions into cell. Calcium leaving the cell is part of a feedback mechanic where the electrical properties of the heart are influenced by calcium concentration in the cytosol. When the concentration begins to change it leads to a phenomena where regular depolarizations of the cell plasma membrane happen; the depolarization

induces spontaneous action potential, causing the L-type Calcium Channels to open. This feed-forward mechanic is another one way coupling which allows for the electrical aspect of the cardiac cell to have an influence on the calcium concentration of the cytosol. These two methods result in a two way coupling between the electrical excitation system and calcium signaling in the cell.

As the CRUs release more calcium into the cytosol, the spike in concentration can trigger neighboring CRUs to open as well possible leading to the cascading effect depicted in Figure 2.2(b). This wave can propagate until the SR stores are depleted of calcium, which are then replenished via an intracellular pump. When calcium begins to pour into the cytosol the concentration begins to rise triggering another even within the cell: calcium release. As calcium diffuses through the cytosol, it reacts with other chemical species; among them, in this model, are the fluorescent dye fluoro-4 and tropomyosin.

The contraction and expansion of the cell's shape is a result of the contractile proteins; the contractile proteins, also called tropomyosin, located in the bottom right-hand corner of Figure 2.2(a), are comprised of troponin, actin, myosin heads, and attached to a sacromere. When calcium binds to the troponin complex the myosin heads are free to converge to the actin bridge; when the myosin heads come in contact with the bridge the striated muscle, the sacromere, that is parallel to the tropomyosin contracts. This myosin contraction is the process through which the cell expands and contracts; when these contractions are performed in unison on a macroscopic scale the pulses. This process of calcium causing heart contractions presents the first coupling between calcium and the contractile nature of a heart cell; these chemical interactions would be called a feed forward process. Once calcium is bound to the complex the bridge like structure deforms causing the rate at which calcium would unbind to decrease. Conceptually the change in the troponin complex causes the bridge to hang onto the calcium for longer.

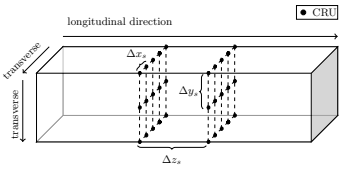

Figure 2.3: The CRUs are modeled in a lattice shape along the z and y axis. The SR, LCCs, and cell membrane are assumed to be everywhere.

In order to represent the shape of the heart cell, as depicted in Figure 2.1(b) mathematically a rectangular prismatic mesh where the CRUs are isotropically spaced throughout the domain as seen in Figure 2.3. The rectangular nature of the mesh and isotropic spacing are unchanged despite the idea of cell contraction; the cells realistically contract but for simplicity the mechanical contraction is implemented as a pseudo-mechanical.

3 Model

In this section, we present the equations of the model along with parameter tables and descriptions of how the equations represent the physiological components. The PDEs of the model are (3.1), (3.2) with $n_{sc} = 3$, (3.3), (3.4) with $n_{ss} = 1$, (3.12), and (3.13). Section 3.1 describes the calcium signaling portion of the model without the presence of electrical excitation or mechanical contraction [5,6], implemented in [3,4]. Section 3.2 introduces the electrical excitation that is connected to the calcium signaling in both the feedforward and feedback directions represented by links ① and ② in Figure 1.1. Link ① from electrical system to the calcium dynamics was first established in [1]. Finally, Section 3.3 completes the fully linked model with the addition of the mechanical contraction component that is also connected to the calcium signaling in both the feedback and feedforward directions represented by links ③ and ④ in Figure 1.1. The effects of cell contraction are implemented via a pseudo-mechanical model, as in [2], which describes force in terms of the proportion of actively connected contractile proteins.

3.1 Calcium signaling

We start with a system of reaction diffusion PDEs

$$\frac{\partial c}{\partial t} = \nabla \cdot (D_c \nabla c) + \sum_{i=1}^{n_{sc}} R_i^{(c)} + (J_{CRU} + J_{leak} - J_{pump}) + \kappa J_{LCC} + J_{m_{leak}} - J_{m_{pump}} \tag{3.1}$$

$$\frac{\partial b_i^{(c)}}{\partial t} = \nabla \cdot (D_{b_i^{(c)}} \nabla b_i^{(c)}) + R_i^{(c)}, \quad i = 1, ..., n_{sc} \tag{3.2}$$

$$\frac{\partial s}{\partial t} = \nabla \cdot (D_s \nabla s) + \sum_{j=1}^{n_{ss}} R_j^{(s)} - \gamma (J_{CRU} + J_{leak} - J_{pump}) \tag{3.3}$$

$$\frac{\partial b_j^{(s)}}{\partial t} = \nabla \cdot (D_{b_j^{(s)}} \nabla b_j^{(s)}) + R_j^{(s)}, \quad j = 1, ..., n_{ss} \tag{3.4}$$

where $c(x,t)$ and $s(x,t)$ represent the concentrations of calcium in the cytosol and SR, respectively. $b_i^{(c)}(x,t)$ and $b_j^{(s)}(x,t)$ represent the concetration of each buffer species in the cytosol SR, respectively. $D_c, D_s, D_{b_i^{(c)}}$, and $D_{b_j^{(s)}}$ are diffusion matrices for Ca^{2+} in the cytosol, Ca^{2+} in the SR, and each buffer species in the cytosol and SR, respectively. While each buffer species programatically possesses a diffusion matrix (following the template of (3.5) and (3.6)), not all species are mobile; hence the diffusion matrices for some species are zero matrices in Table 3.1.

The reaction terms $R_i^{(c)}$ and $R_j^{(s)}$ describe the reactions between cytosolic Ca^{2+} and each cytosolic buffer species, and the reactions between SR Ca^{2+} and each SR buffer species

$$R_i^{(c)} = -k^+_{b_i^{(c)}}\, c\, b_i^{(c)} + k^-_{b_i^{(c)}} \left(b^{(c)}_{i,total} - b_i^{(c)}\right), \quad i = 1, ..., n_{sc} \tag{3.5}$$

$$R_j^{(s)} = -k^+_{b_j^{(s)}}\, s\, b_j^{(s)} + k^-_{b_j^{(s)}} \left(b^{(s)}_{j,total} - b_j^{(s)}\right), \quad j = 1, ..., n_{ss}. \tag{3.6}$$

The points of connection between (3.1) and (3.2), and between (3.3) and (3.4), are these reaction terms (3.5) and (3.6). The amounts of "free" calcium ions, $c(x,t)$ and $s(x,t)$, and of "free" buffer species, are determined by these reactions: whatever has not been bound by a reaction is the concentration remaining. In the cytosol, two buffer species are considered: a fluorescent dye, $b_1^{(c)}(x,t)$, and a contractile protein troponin, $b_2^{(c)}(x,t)$. We will revisit the subject of troponin in our extension of this model to include the pseudo-mechanical dynamics of the cell. In the SR, a single buffer species is considered: calsequestrin, $b_1^{(s)}(x,t)$, a calcium-binding protein which helps maintain the SR calcium reserves at a much higher concentration than the cytosol (i.e., prevents too great a loss through diffusion).

The flux terms J_{CRU}, J_{leak} and J_{pump} describe the calcium-induced release of Ca^{2+} into the cytosol from the SR, the continuous leak of Ca^{2+} into the cytosol from the SR, and the pumping of Ca^{2+} back into the

Table 3.1: Parameter values for calcium signaling: PDEs.

Parameters	Definition	Values/Units
$c(x,t)$	cytosol calcium concentration	μM
$s(x,t)$	SR calcium concentration	μM
n_{sc}	number of cytosol Ca^{2+} buffer species	2
n_{ss}	number of SR Ca^{2+} buffer species	1
${b_1^{(c)}}_{total}$	total amount of $b_1^{(c)}(x,t)$, dye, in cytosol	50 μM
${b_2^{(c)}}_{total}$	total amount of $b_2^{(c)}(x,t)$, troponin, in cytosol	123 μM
${b_1^{(s)}}_{total}$	total amount of $b_1^{(s)}(x,t)$, calsequestrin, in SR	6000 μM
D_c	cytosolic calcium diffusion coefficient matrix	diag(0.15, 0.15, 0.3)
D_s	SR calcium diffusion coefficient matrix	diag(0.78, 0.78, 0.78) μm^2/ms
$D_{b_1^{(c)}}$	cytosol buffer diffusion coefficient matrix ($i=1$, dye)	diag(0.01, 0.01, 0.02) μm^2/ms
$D_{b_2^{(c)}}$	cytosol buffer diffusion coefficient matrix ($i=2$, troponin)	diag(0.00, 0.00, 0.00) μm^2/ms
$D_{b_1^{(s)}}$	SR buffer diffusion coefficient matrix ($i=1$, calsequestrin)	diag(0.00, 0.00, 0.00) μm^2/ms
$R_i^{(c)}, R_j^{(s)}$	reactions of cytosol, SR Ca^{2+} with buffers	μM/ms
$k^+_{b_1^{(c)}}$	forward reaction coefficient for $b_1^{(c)}$, dye	80e-3 μM/ms
$k^+_{b_2^{(c)}}$	forward reaction coefficient for $b_2^{(c)}$, troponin	100e-3 μM/ms
$k^+_{b_1^{(s)}}$	forward reaction coefficient for $b_1^{(c)}$, calsequestrin	39.0e-3 μM/ms
$k^-_{b_1^{(c)}}$	reverse reaction coefficient for $b_1^{(c)}$, dye	90e-3 ms^{-1}
$k^-_{b_2^{(c)}}$	reverse reaction coefficient for $b_2^{(c)}$, troponin	100e-3 ms^{-1}
$k^-_{b_1^{(s)}}$	reverse reaction coefficient for $b_1^{(s)}$, calsequestrin	78 ms^{-1}
γ	ratio of volume of cytosol to SR	14

SR from the cytosol. $J_{LCC}, J_{m_{leak}}$, and $J_{m_{pump}}$ describe the fluxes of calcium into and out of the cell via the plasma membrane. The coupling between (3.1) and (3.3) is achieved by the three flux terms shared by both. J_{pump} and J_{leak} are functions only of cytosol calcium $c(x,t)$; J_{CRU} has an additional dependence on SR calcium $s(x,t)$. $J_{LCC}, J_{m_{leak}}$, and $J_{m_{pump}}$ describe the fluxes of calcium into and out of the cell via the plasma membrane. J_{pump} replenishes the calcium stores in the SR; it increases SR calcium concentration by decreasing cytosol calcium concentration. J_{leak} is a continuous leakage of those SR calcium stores into the cytosol; it increases cytosol concentration by decreasing SR calcium concentration. In the absence of sparking (i.e., when J_{CRU} is inactive, or 0) J_{pump} and J_{leak} balance each other to keep the levels of $c(x,t)$ and $s(x,t)$ relatively consistent

$$J_{pump}(c) = V_{pump}\left(\frac{c^{n_{pump}}}{K_{pump}^{n_{pump}} + c^{n_{pump}}}\right) \tag{3.7}$$

$$J_{leak} = J_{pump}(c_0). \tag{3.8}$$

J_{pump}, a function of cytosolic calcium $c(x,t)$, consists of the the maximum pump velocity V_{pump} multiplied against the relationship between $c(x,t)$ and the pump sensitivity K_{pump}; the superscript n_{pump} refers to the Hill coefficient (quantifying the degree of cooperative binding) for the pump function. This has the practical effect of multiplying the maximum possible pump velocity against a number between 0 and 1, exclusive. J_{leak}, which continuously leaks calcium into the cytosol from the SR, is simply J_{pump} evaluated at the basal cytosolic calcium concentration c_0. As noted, J_{pump} balances J_{leak} in the absence of sparking. However, it can and does balance J_{CRU} as well under conditions of active calcium release.

J_{CRU} is the Ca^{2+} flux into the cytosol from the SR via each individual point source at which a CRU has

Table 3.2: Parameter values for calcium signaling: coupling by pump and leak.

Parameters	Definition	Values/Units
c_0	initial cytosol calcium concentration	0.1 μM
J_{pump}	calcium transfer from cytosol to SR	μM/ms
J_{leak}	calcium leak from SR	μM/ms
V_{pump}	maximum pump rate	2 to 6 μM/ms
K_{pump}	pump sensitivity to Ca^{2+}	0.184 μM
n_{pump}	Hill coefficient for pump function	4.0

Table 3.3: Parameter values for calcium signaling: coupling by sparking.

Parameters	Definition	Values/Units
s_0	initial SR calcium concentration	1,000 to 10,000 μM
J_{CRU}	calcium flux from SR to cytosol via CRUs	μM/ms
$\mathcal{O}$	gating function for J_{CRU}	1
J_{prob}	probability of CRU opening	0 to 1
$\mathbf{x}$	three-dimensional vector for CRU location	μm
$\hat{\sigma}$	maximum rate of release	100 to 200 μMμm^3/ms
u_{rand}	uniformly distributed random variable	0 to 1
n_{prob}	Hill coefficient for probability function	1.6
P_{max}	maximum probability for release	0.3
K_{prob_c}	sensitivity of CRU to cytosol calcium	5 to 15 μM
K_{prob_s}	sensitivity of CRU to SR calcium	200 to 550 μM
$\delta(\mathbf{x}-\hat{\mathbf{x}})$	Dirac delta distribution	0, 1

been assigned. It can be considered as the product of three segments

$$J_{CRU}(c,s,\mathbf{x},t) = \sum_{\hat{\mathbf{x}}\in\Omega_s}\left(\hat{\sigma}\Big(\frac{s-c}{s_0-c_0}\Big)\right)\mathcal{O}(c,s)\,\delta(\mathbf{x}-\hat{\mathbf{x}}) \tag{3.9}$$

$$\mathcal{O}(c,s) = \left\{\begin{array}{ll} 1 & \text{if } u_{rand}\le J_{prob} \\ 0 & \text{if } u_{rand} > J_{prob}\end{array}\right\} \tag{3.10}$$

$$J_{prob}(c,s) = P_{max}\left(\frac{c^{n_{prob}}}{K_{prob_c}^{n_{prob}}+c^{n_{prob}}}\right)\left(\frac{s^{n_{prob}}}{K_{prob_s}^{n_{prob}}+s^{n_{prob}}}\right). \tag{3.11}$$

First, similarly to how in J_{pump} the maximum pump rate is scaled against the concentration of available cytosol calcium, the maximum rate of Ca^{2+} release $\hat{\sigma}$ is here scaled against the ratios of calcium concentrations in the cytosol and in the SR.

Second, following the same pattern a maximum value multiplied against some scaling proportion between 0 and 1 the gating function $\mathcal{O}$ has the practical effect of "budgeting" the calcium SR stores such that when the stores are low, the given CRU becomes much less likely to open; each CRU is assigned a uniformly distributed random value, which is compared to the single value returned by the CRU opening probability J_{prob} to determine whether or not the given CRU will open.

Third, the Dirac delta distribution models each CRU as a point source for calcium release.

3.2 Electrical excitation

The membrane potential of the cell depends on both the cytosol calcium ion concentration and also on the cytosol potassium ion (K^+) concentration. While a complete description of the relationship between electrolytes and membrane potential is beyond the scope of this paper [2, 7], note the ω term, an addition of our model which introduces a dependency on c to complete the coupling between the electrical and chemical systems.

The Ca^{2+} conductance is much faster than the K^+ conductance, and so the calcium conductance can be approximated as m_∞ or instantaneously steady-state at all times; the potassium conductance requires a

separate description (3.13)

$$\frac{\partial V}{\partial t} = \tau \frac{1}{C}\Big(I_{\text{app}} - g_L(V - V_L) - g_{Ca}\, m_\infty(V)\,(V - V_{Ca}) - g_K\, n\,(V - V_K) + \omega\,(J_{m_{pump}} - J_{m_{leak}})\Big) \tag{3.12}$$

$$\frac{\partial n}{\partial t} = \tau\, \lambda_n(V)\,[n_\infty(V) - n]. \tag{3.13}$$

The connection between (3.1) and (3.12), the link from the electrical system to the chemical system, comes through J_{LCC}, the only calcium flux term to involve voltage. Note the parameter κ, which is an external scaling factor for J_{LCC} rather than an intrinsic physiological component; if the value of κ is set to 0, the connection is effectively switched off, and the calcium dynamics are then modelled as though voltage were not involved

$$J_{LCC} = \frac{S\, g_{Ca}\, m_\infty\,(V - V_{Ca})}{2F}. \tag{3.14}$$

S, the surface area of the cell, is included in light of the fact that J_{LCC} describes the influx of calcium through L-type calcium channels (LCCs), which are present in the enclosing plasma membrane of the cell: the surface area of the cell is the surface area of the membrane.

We model the effect of cytosol calcium concentration on voltage by treating the calcium efflux term $(J_{m_{pump}} - J_{m_{leak}})$ as equivalent to the sodium-calcium exchanger current: we are thus able to describe the current generated by the sodium-calcium exchange as a function of simple calcium loss.

The individual components of the calcium efflux term are near-duplicates in form of the earlier J_{pump} (3.7) and J_{leak} (3.8). As J_{pump} described the removal of calcium from the cytosol and its transfer into SR stores, $J_{m_{pump}}$ describes the removal of calcium from the cytosol and its transfer to outside the cell across the membrane. J_{leak} described a gradual leak of calcium into the cytosol from the SR; J_{CRU} described an abrupt, high-concentration (high relative to the leak) release of calcium into the cytosol from the SR. Similarly, $J_{m_{leak}}$ describes a gradual leak of calcium into the cytosol from outside the cell via the plasma membrane, while J_{LCC} describes a sudden spike of calcium release into the cytosol via the LCCs

$$J_{m_{pump}}(c) = V_{m_{pump}}\Big(\frac{c^{m_{n_{pump}}}}{K_{m_{pump}}^{m_{n_{pump}}} + c^{m_{n_{pump}}}}\Big) \tag{3.15}$$

$$J_{m_{leak}} = J_{m_{pump}}(c_0). \tag{3.16}$$

At this juncture, we extend the model to connect the chemical system to the electrical system via the inclusion of the current generated by calcium leaving the cell via $J_{m_{pump}}$ and $J_{m_{leak}}$, which directly affects the voltage. We collect and incorporate these as a single term, the calcium efflux $(J_{m_{pump}} - J_{m_{leak}})$, and introduce ω as a parameter for feedback strength, a scaling factor with the same essential function as κ in (3.1): if it is set to 0, the only terms of (3.12) which depend on the cytosolic calcium concentration drop out, and the connection from calcium signaling to electrical excitation is severed.

3.3 Pseudo-mechanical contraction

We complete the proposed linkages of the model by introducing feedback and feed-forward terms for the contractile dynamics. We describe this as "pseudo-mechanical" because the domain itself is unchanged; in our model, the physical dimensions of the cell and the locations of the CRUs do not alter. We instead model the contraction via the proportion of contractile proteins which have bound to calcium and changed shape as a result, which generates the force required for cell contraction.

The contractile proteins in question, though considered as a single species, are the combination of actin and myosin when linked via cross-bridges. This linkage is made possible by Ca^{2+} binding to troponin, the cytosol buffer species $b_2^{(c)}(x,t)$: it is this binding that allows the actin-myosin cross-bridges to form. We therefore introduce a new cytosol species, $b_3^{(c)}(x,t)$, to describe these actin-myosin cross-bridges, and

Table 3.4: Parameter values for electrical excitation: gating functions and membrane potential.

Parameters	Definition	Values/Units
τ	scaling factor to fit action potential duration	0.1 μM μm^3/ms
$V(x,t)$	membrane potential (voltage)	mV
V_L	equilibrium potential for leak conductance	-50 mV
V_{Ca}	equilibrium potential for Ca^{2+} conductance	100 mV
V_K	equilibrium potential for K^+ conductance	-70 mV
C	membrane capacitance	20 μF/cm^2
I_{app}	applied current	10 μA/cm^2
g_L	maximum/instantaneous conductance for leak	2 mmho/cm^2
g_{Ca}	max./instantaneous conductance for Ca^{2+}	4 mmho/cm^2
g_K	max./instantaneous conductance for K^+	8 mmho/cm^2
m_∞	fraction of open calcium channels at steady state	0 to 1
$n(x,t)$	fraction of open potassium channels	0 to 1
n_∞	fraction of open potassium channels at steady state	1
$\lambda_n(V)$	rate constant for opening of K^+ channels	s^{-1}
J_{LCC}	influx of calcium into cell via L-type calcium channels	μM/ms
S	surface area of the cell	3604.48 μm
F	Faraday constant	95484.56 C/mol
κ	scaling factor of J_{LCC}	0.01
ω	feedback strength (scaling factor) for Ca^{2+} efflux	μA ms/μM cm^2
$J_{m_{pump}}$	pump of calcium out from cell via L-type calcium channels	μM/ms
$J_{m_{leak}}$	leak of calcium out from cell via L-type calcium channels	μM/ms
$V_{m_{pump}}$	maximum pump rate	1 μM/ms
$m_{n_{pump}}$	membrane pump Hill coefficient	2
$K_{m_{pump}}$	membrane pump sensitivity	0.18

construct a third cytosol reaction term:

$$R_{b_3}^{(c)} = -k^+_{b_3^{(c)}} \left(\frac{b_{2,total}^{(c)} - b_2^{(c)}}{b_{2,total}^{(c)}}\right)^2 b_3^{(c)} + k^-_{b_3^{(c)}} (b_{3,total}^{(c)} - b_3^{(c)}). \tag{3.17}$$

Notice that this is not the same as the generic pattern for buffer species reaction terms from the initial model. There is no immediately clear dependence on cytosolic calcium $c(x,t)$. However, while $c(x,t)$ is not explicitly included, it is present in the proportion involving troponin, $b_3^{(c)}(x,t)$, which itself depends explicitly on cytosol calcium levels; $R_{b_3}^{(c)}$, like the other two reaction equations, does in fact depend on cytosol calcium concentration.

We modify the reaction equation for troponin as well. When troponin binds to Ca^{2+}, the protein as a whole, as noted, changes shape: not only does this allow actin-myosin cross-bridges to form, but it also traps the calcium in its connection to the troponin so that the disassociation rate decreases dramatically. To account for this, we add a shortening factor ε to describe how the separation of troponin and calcium has been physically, not chemically, impaired. Note, again, that $R_{b_2}^{(c)}$ remains a function of cytosol calcium concentration $c(x,t)$

$$R_{b_2}^{(c)} = -k^+_{b_2^{(c)}} c\, b_2^{(c)} + k^-_{b_2^{(c)}} \left(b_{2,total}^{(c)} - b_2^{(c)}\right)\frac{1}{\varepsilon} \tag{3.18}$$

$$\varepsilon = \exp\left(F_{max}\, k_s \left(\frac{b_{3,total}^{(c)} - b_3^{(c)} - [XB]_0}{b_{3,total}^{(c)} - [XB]_0}\right)\right). \tag{3.19}$$

This shortening factor refers back to the concentration of $b_3^{(c)}(x,t)$, the actin-myosin cross-bridges, and to the force that their linkage generates. It is scaled by the maximum possible contractile force F_{max}, the actin stiffness k_s, and the proportion of active to inactive actin-myosin cross-bridges. Like ω and κ, ε is our point of control over the linkage between systems: if the exponent is 0, the overall value simply turns to 1, and $R_{b_2}^{(c)}$ reverts to its earlier form (3.5).

Table 3.5: Parameter values for mechanical contraction: new cytosol species reactions.

Parameters	Definition	Values/Units
$b_3^{(c)}(x,t)$	inactive actin-myosin cross-bridges [X]	μM
$[XB]$	active (linked) actin-myosin cross-bridges	μM
$[XB]_0$	initial concentration of active cross-bridges	μM
$k^+_{b_3^{(c)}}$	forward reaction coefficient for $b_3^{(c)}(x,t)$, actin-myosin cross-bridges	0.04 ms^{-1}
$k^-_{b_3^{(c)}}$	reverse reaction coefficient for $b_3^{(c)}(x,t)$, actin-myosin cross-bridges	0.01 ms^{-1}
ε	shortening factor	0 to 1
k_s	stiffness of actin filament	0.025 N/m
F_{max}	maximum force generated by actin-myosin crossbridges	120 μN

The addition of these two reaction terms connects the three components of our model. The calcium signaling is linked to the pseudo-mechanical contraction through the cross-bridge term, and the pseudo-mechanical contraction is in turn connected to the calcium signaling through the inclusion of the cytosol calcium concentration in the modified reaction equation for troponin. Thus all links in Figure 1.1 are established and thus the three components of the model are fully linked.

Table 4.1: Parameters for the ODE, linear, nonlinear solvers.

parameters	ODE	Nonlinear	Linear
methodname	NDF	Newton	BiCGSTAB
maxorder	5		
reltol	10^{-6}	10^{-4}	10^{-6}
Nx,Ny,Nz	33,33,129		
Nx,Ny,Nz(out)	33,33,129		
dtmin,dtmax,dtini	-20,0.500,0.500		
dtout,nsout,ityput	1.0,1,0		
diagoutput	0	0	0
maxit		4	50
initguess		p	
stopping		ode15s	
enforcenonneg		no	
epsclip		10^{-14}	
tolrelres			10^{-2}
abstol	10^{-8}		10^{-8}
maxnsteps	999999		

4 Numerical Method

In order to address our problem we need to solve a system of time dependent parabolic partial differential equations. These PDEs are coupled by non-linear reaction and source terms. The domain in our model is a rectangular prism, which correlates to the brick shape of a heart cell.

We use a method of lines (MOL) approach to spatially discretize this model. We use the finite volume method (FVM) for spatial discretization. The result of this spatial discretization is a large system of ordinary differential equations (ODEs). A method of lines discretization of diffusion-reaction equations with second-order spatial derivatives results necessarily in a stiff ODE system, since the time step size restrictions due to the CFL condition are considered too severe to allow for explicit time-stepping methods. This necessitates the use of a sophisticated ODE solver such as the family of numerical differentiation formulas (NDFk). Our stiff ODEs, which requires an implicit ODE method, are then taken and transformed in to non-linear equations and are then solved with the TMP. These non-linear equations are then transformed into linear equations, these are solved with the BiCGSTAB iteration method.

The spatial discretization of the application problem with $n_s = 8$ species using the finite volume method with N control volumes. The result is a system of non-linear ordinary differential equations (ODEs) with the number of degrees of freedom (DOF), $n_{eq} = n_s\, N$. We are using a matrix free method that helps with memory allocation, thus allowing to have efficient memory management.

The implementation of this model is done in C using Message Passing Interface (MPI) to parallelize. Parallelization is to block-distribute all large arrays to all MPI processes. MPI commands such as `MPI_Isend` and `MPI_Irecv`, which are non-blocking MPI communications commands, sent messages between neighboring processes. `MPI_Allreduce` is used in the computation of scale products.

5 Results

We present a full model of the calcium dynamics of a heart cell, which is an extension of [1]. To visualize the solutions, we conduct numerical simulations to examine the behavior. For each behavior, we present four figures: line-scans/voltage plots, iso surface plots, CRU open plots, and SR plots. Line-scans are produced by tracking the concentration of the cystolic Ca^{2+} concentration along the center of the cell at each millisecond. The concentrations of Ca^{2+} are plotted on a two-dimensional domain for each second, and then overlayed upon each other producing the final image. Higher concentrations of Ca^{2+} are indicated by red, while lower concentrations are indicated by blue. Voltage plots track the average voltage at the center of the cell domain, and then is plotted versus time. Iso surface plots show the concentration of Ca^{2+} in the cytosol. Blue represents the lowest value of of Ca^{2+} concentration we choose to track, which is 65 μM. Higher concentrations are indicated by a yellow-ish color. CRU plots show the open calcium release units, which are represented by blue dots in the three dimensional representation. SR plots show the concentration of Ca^{2+} in the SR as it relates to the right, center, and left of the cell. All simulations are run for 1000 ms.

In Section 5.1, we present results of one-way coupling between electrical excitation and calcium signaling, which produce two general phenomenon: sparking and transient blow-up. One-way coupling is achieved by only considering the forward connection between the electrical and calcium systems, as seen in Figure 1.1. In Section 5.2, we present results of a two-way coupling between the calcium and electrical systems. In two way coulping, we consider both the feedforward and feedback connectiion between the electrical and calcium systems. As descrbed in Section 3, two-way coupling is mathematically achieved through the inclusion of a calcium efflux term, scaled by the factor ω, referred to as a feedback strength coefficient. We present a paramater study of ω in which we examine how varying the value impacts the behavior of our solutions.

5.1 Electrical Excitation to Calcium Signaling: One-Way Coupling

5.1.1 Blow-up

The first case we present is periodic blow-up. A case is classified as blow-up when there are quick Ca^{2+} releases into the cell at significantly high levels, without returning to base level. In periodic blow-up, we experience similar behavior, but calcium is returns to basal level, before returning to the same behavior. This periodic behavior can be examined in Figures 5.1–5.3. In Figure 5.1 as time progresses, we observe a large number of calcium release units opening, culminating at $t = 250$ ms, when the entire domain is filled with CRUs. This signifies that a large amount of calcium is being dumped into the cytosol of the cell. In Figure 5.2, we observe that the concentration of Ca^{2+} reaches significantly high levels evident through the large amount of yellow, but returns to a lower, but still elevated level at $t = 250$ ms. The accompanying line-scan in Figure 5.3 (a), shows period influxes of high Ca^{2+} concentrations, which repeats until $t = 400$ ms, when the Ca^{2+} dips so low, it barely registers. In Figure 5.3 (b), we observe the average voltage. There are influxes of electrical pulses into the system at $t = 250$ ms and $t = 900$ ms. We see that although we have pulses entering the system, the calcium releases seems to be unaffected.

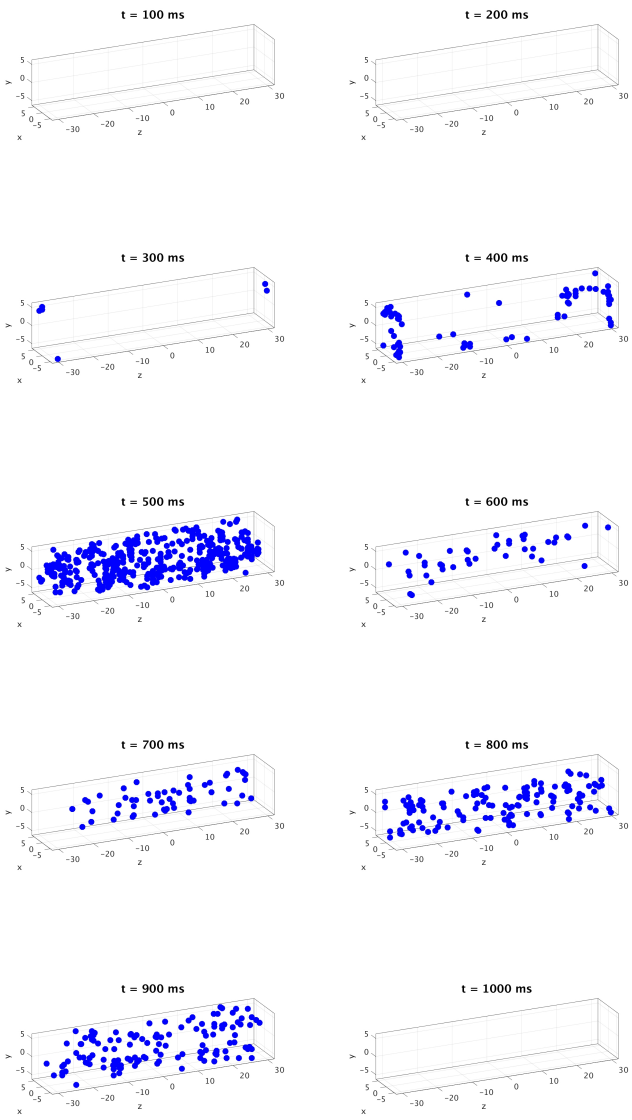

Figure 5.1: CRU open plots for blow-up with $\omega = 0$.

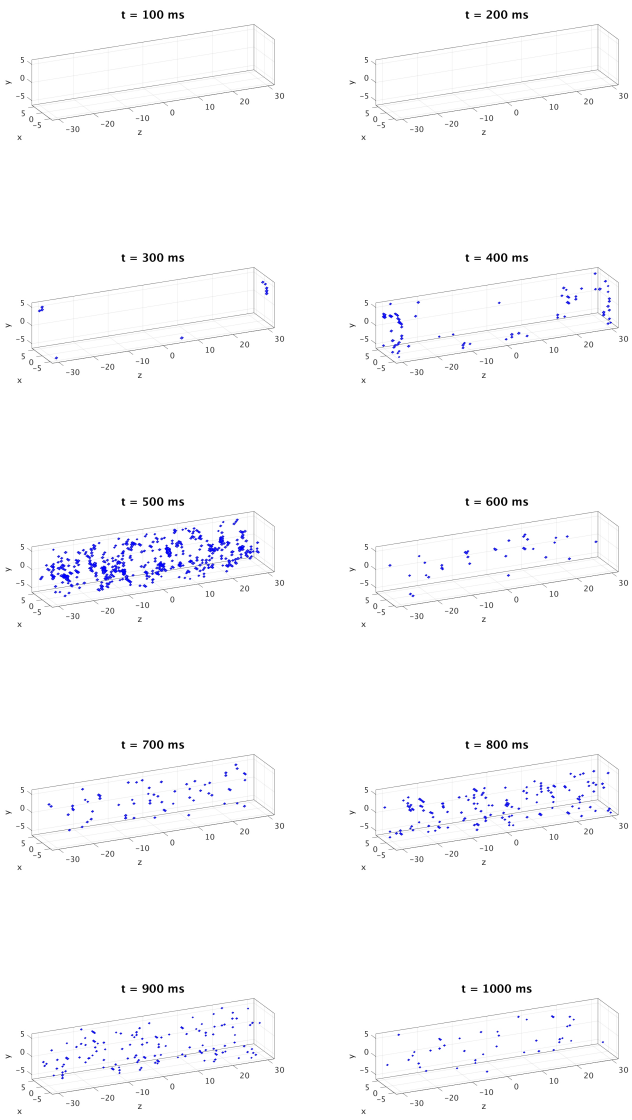

Figure 5.2: ISO open plots for blow-up with $\omega = 0$.

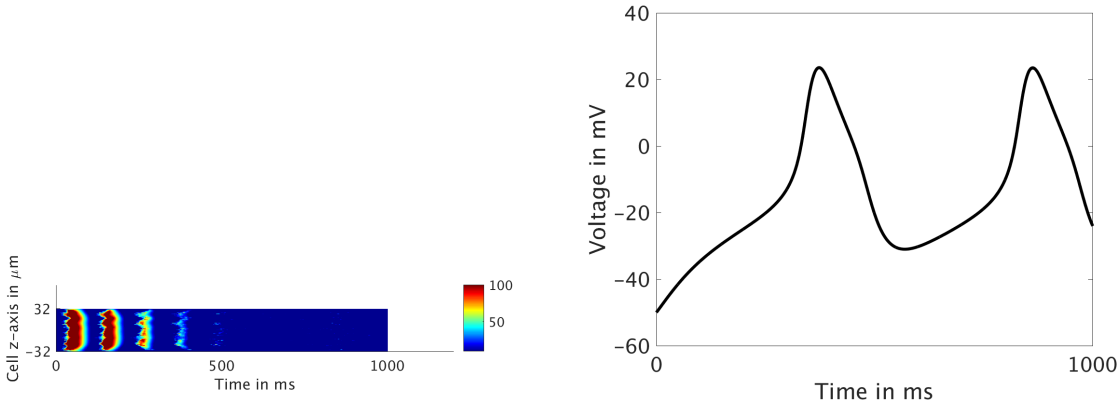

Figure 5.3: Voltage plot for a blow-up with $\omega = 0$

5.1.2 Wave

The second behavior observed is light sparking in Figures 5.4–5.6. Light sparking is defined as a small releases of Ca^{2+} observed throughout the domain. Although there is sparking, it does not trigger any further physiollogical behavior such as wave generation or blow-up. As observed in Figure 5.4, we see only a small amount of CRUs opening as time increases. This behavior is also observed in Figure 5.5, as we only a small amount of points of Ca^{2+}. We use a line-scan to visualize the behavior of the system as a two dimensional representation in Figure 5.6.

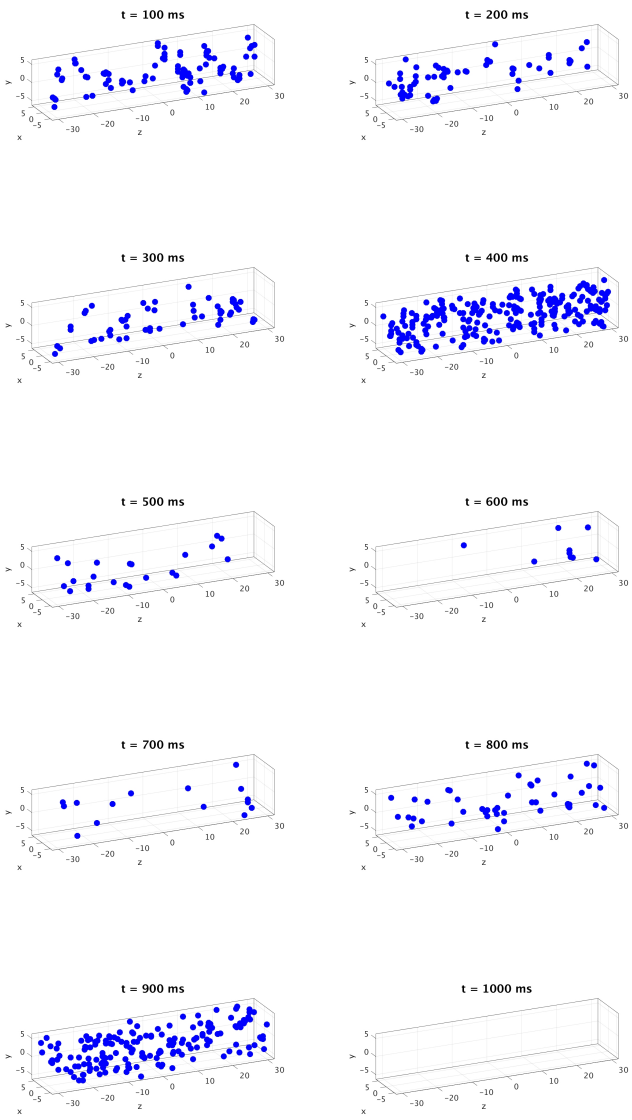

Figure 5.4: CRU open plots for wave with $\omega = 0$.

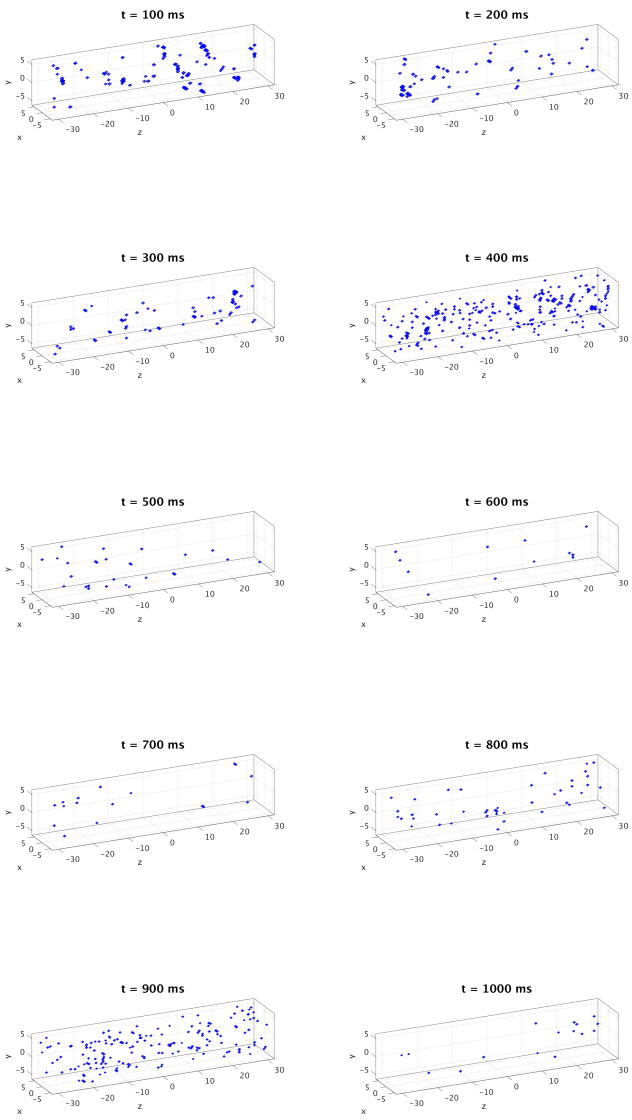

Figure 5.5: ISO open plots for wave with $\omega = 0$.

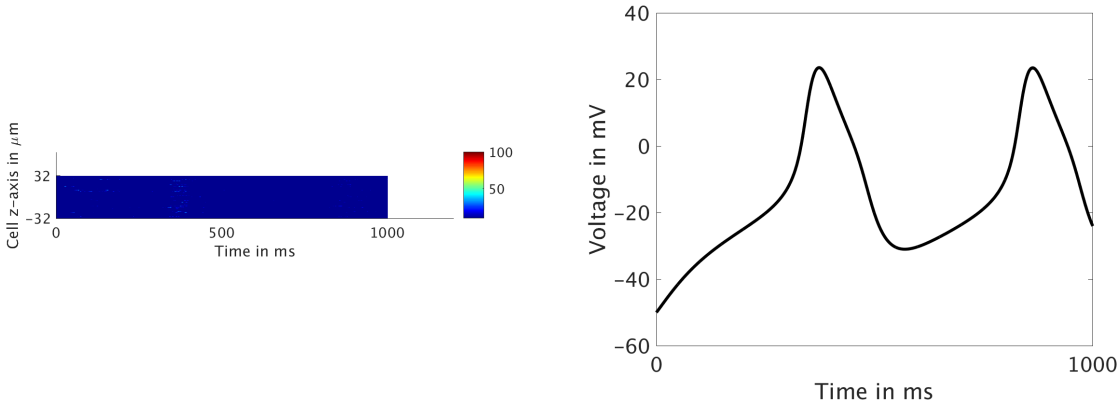

Figure 5.6: Voltage plot for a wave with $\omega = 0$

5.1.3 Heavy Sparking

The last behavior we observe is heavy sparking in Figures 5.7–5.9. Compared to light sparking, heavy sparking is denoted by a higher concentration of Ca^{2+} observed throughout the cell. In Figure 5.7, a higher number of CRUs are opening as time increases. Figure 5.8 confirms the higher concentration of Ca^{2+} by showing parts of the cell as being yellow, which is inidcative of a high concentration; lower concentrations are denoted by blue. The accompanying line-scan in Figure 5.9 shows a high concentration of Ca^{2+}, evident through the larger amount of places which show light blue or red colors.

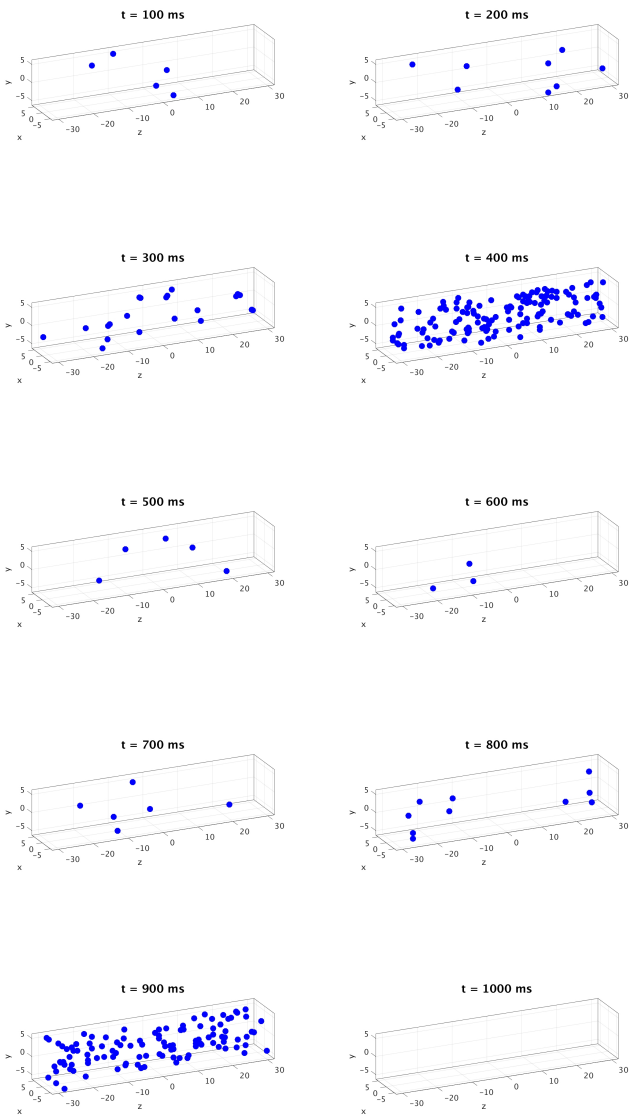

Figure 5.7: CRU open plots for spark with $\omega = 0$.

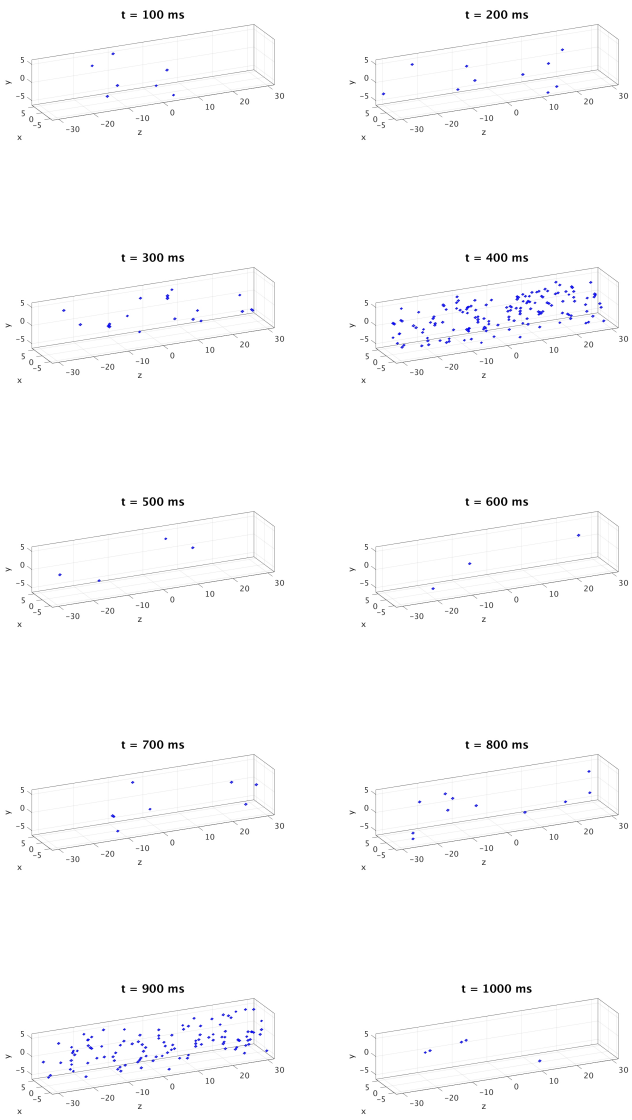

Figure 5.8: ISO open plots for spark with $\omega = 0$.

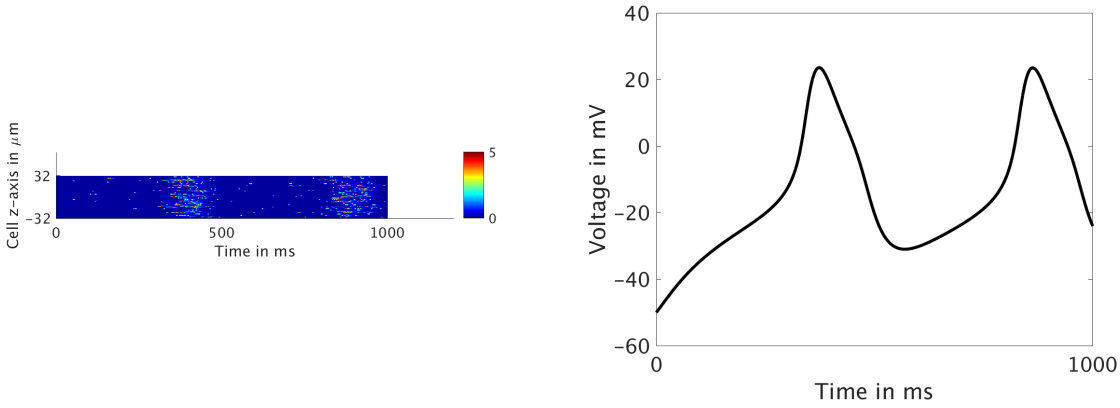

Figure 5.9: Lscan and voltage plot for spark with $\omega = 0$

5.2 Electrical Excitation and Calcium Signaling: Two Way Coupling

We consider five cases of ω to test the feedback strength between calcium signaling and electrical excitation: $\omega = 10, 30, 50$ and $, 100$.

5.2.1 Blow-up

We consider five cases of ω and present line-scans, voltage plots, and SR plots to examine the impact each value has on the solutions. While line-scans appear similar, there is a clear distinction. As in Section 4.1, we experience a periodic blow-up. If $\omega = 0$, the same behavior is observed as in Figure 5.3. As we increase ω, the periodicity of the blow-ups continue for a longer amount of time. If we examine the accompanying voltage plots, we observe that as ω increases, so does the amount of voltage entering the system. Beginning at $\omega = 50$, we observe a behavior known as early afterdepolarization or EAD. This occurs when an increase of voltage frequency is observed before the previous polarization of influx of voltage is complete. An amalgamation of these behaviors in multiple cardiomyocytes could result in cardiac arrhythmias. SR plots show the amount of Ca^{2+} in the SR. We observe that as ω increases, the amount of Ca^{2+} is being removed (or pumped out) increases.

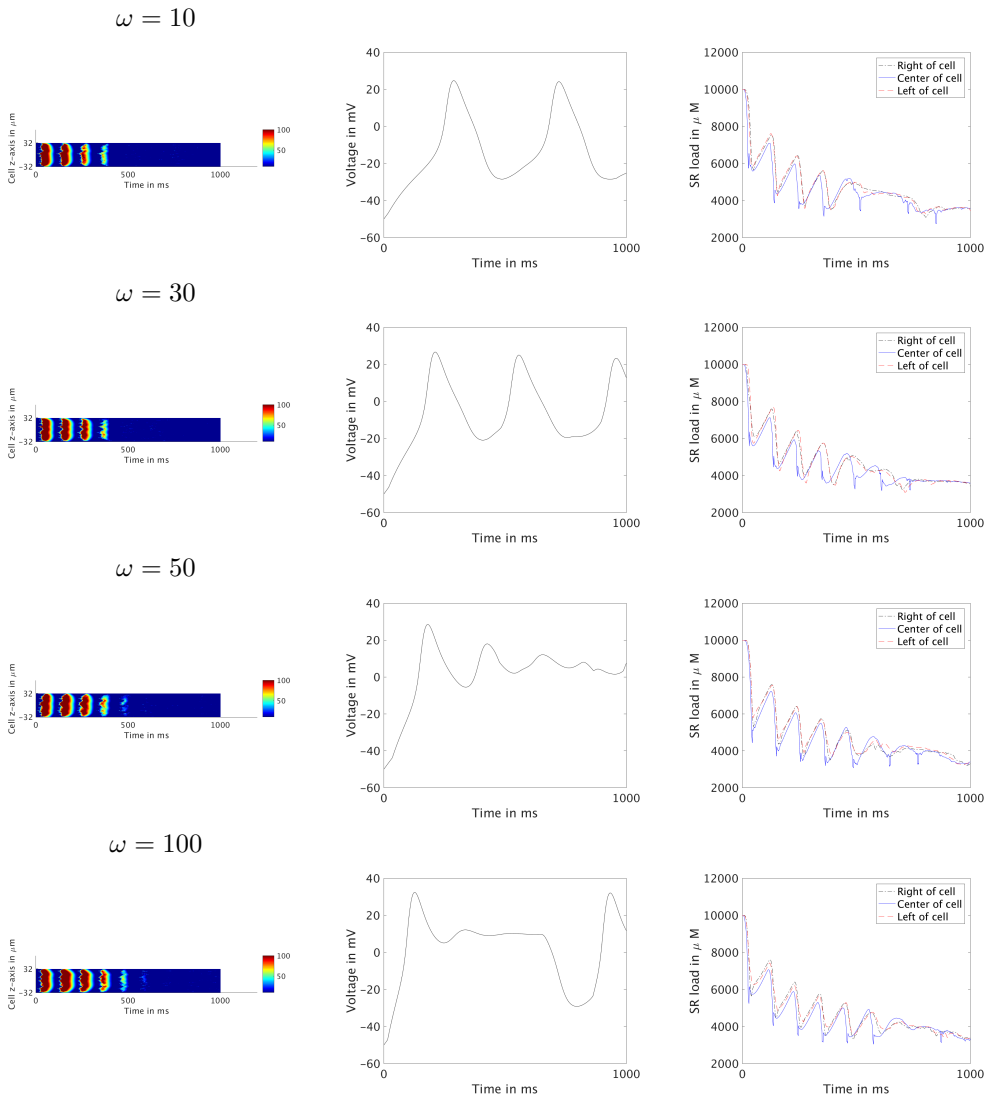

Figure 5.10: Line-scans, voltage plots, and SR plots for blow-up with $\omega = 10, 30, 50$, and 100.

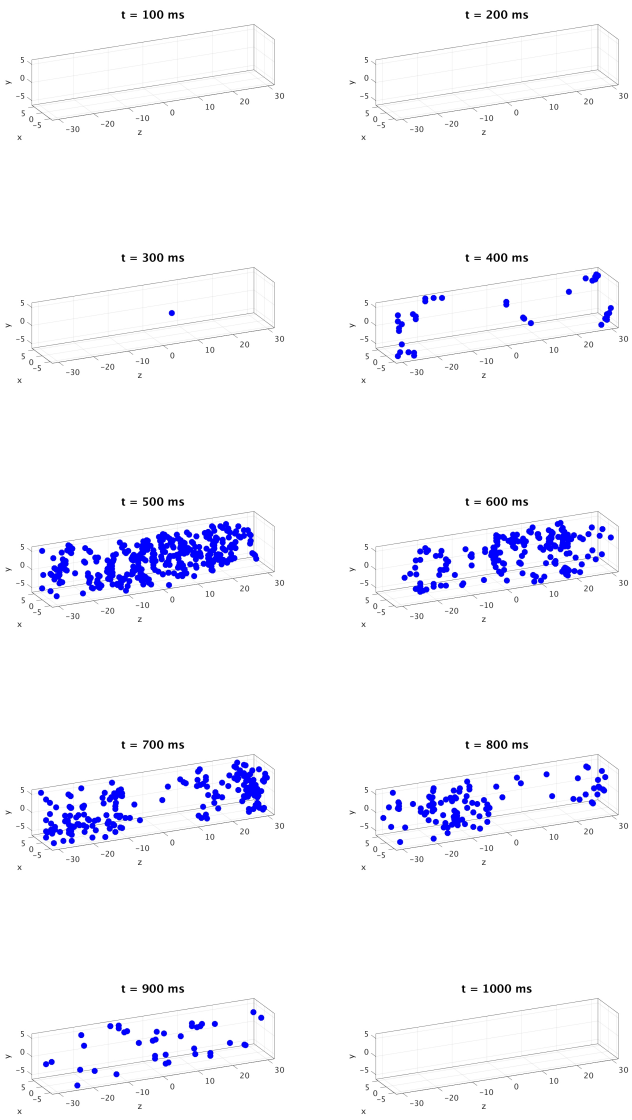

Figure 5.11: CRU open plots for blow-up with $\omega = 30$.

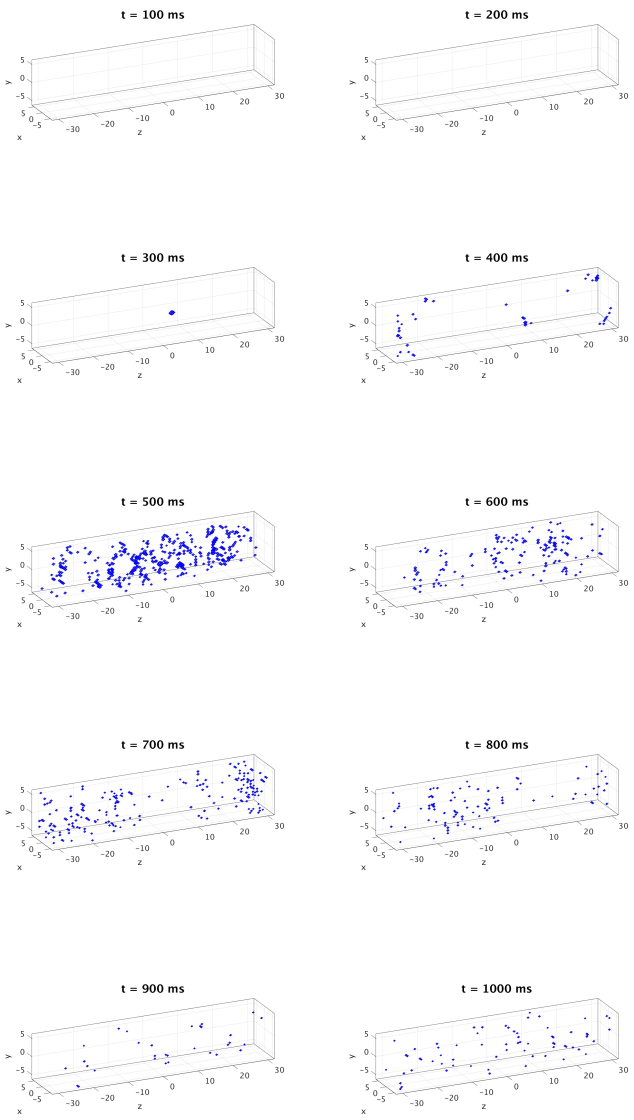

Figure 5.12: ISO open plots for blow-up with $\omega = 30$.

5.2.2 Wave

We continue with analysis of the second case for ω testing: light sparking. As observed in Section 4.1, we observe a light sparking, yet the effect of ω can be seen. In Figure 4.16, as ω increases, the amount of small releases of Ca^{2+} increases. Although we do not reach a heavy sparking case, a higher concentration is observed. Examining the accompanying voltage plots shows similar behavior; there are periodic influxes of voltage though the system. Unlike in the blow-up case, we experience no early afterdepolarization.

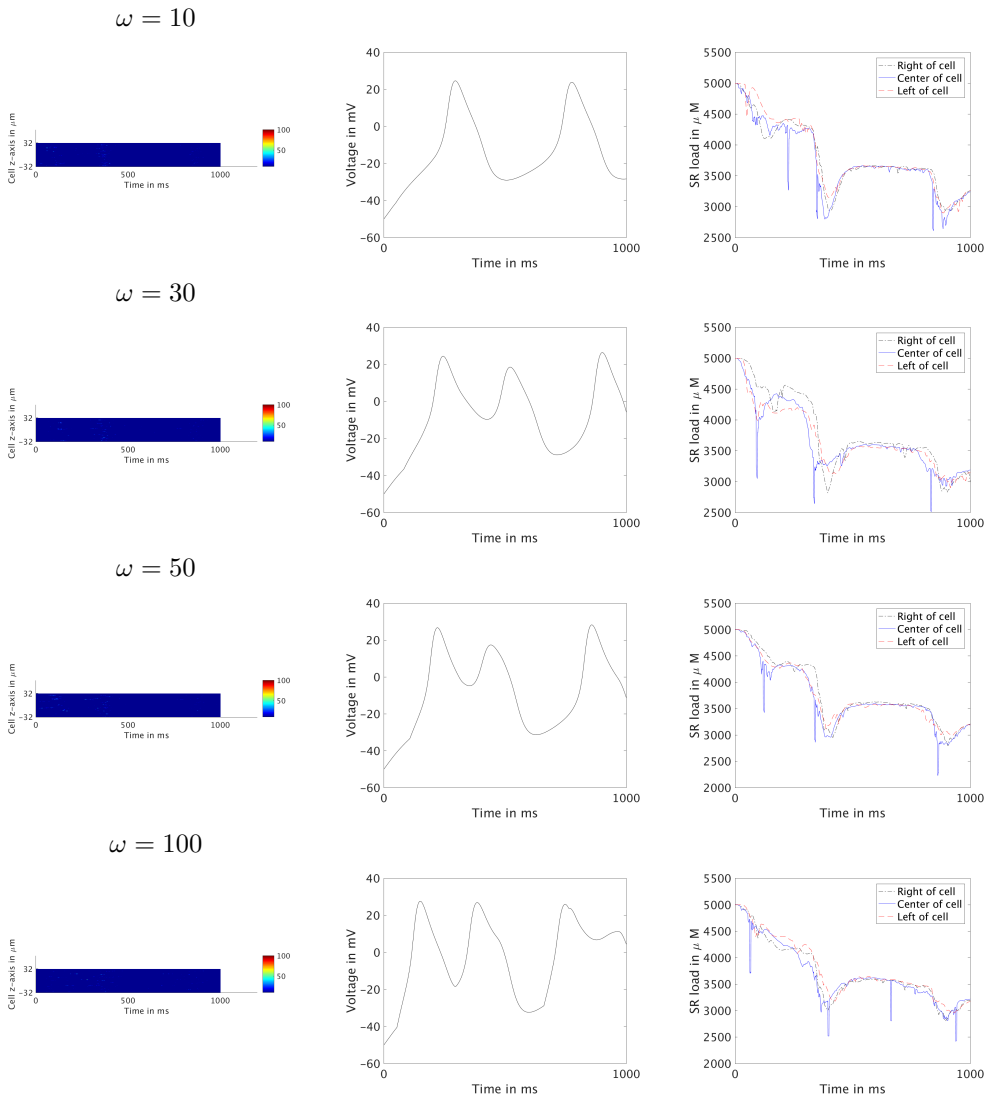

Figure 5.13: Line-scans, voltage plots, and SR plots for a wave with $\omega = 10, 30, 50$, and 100.

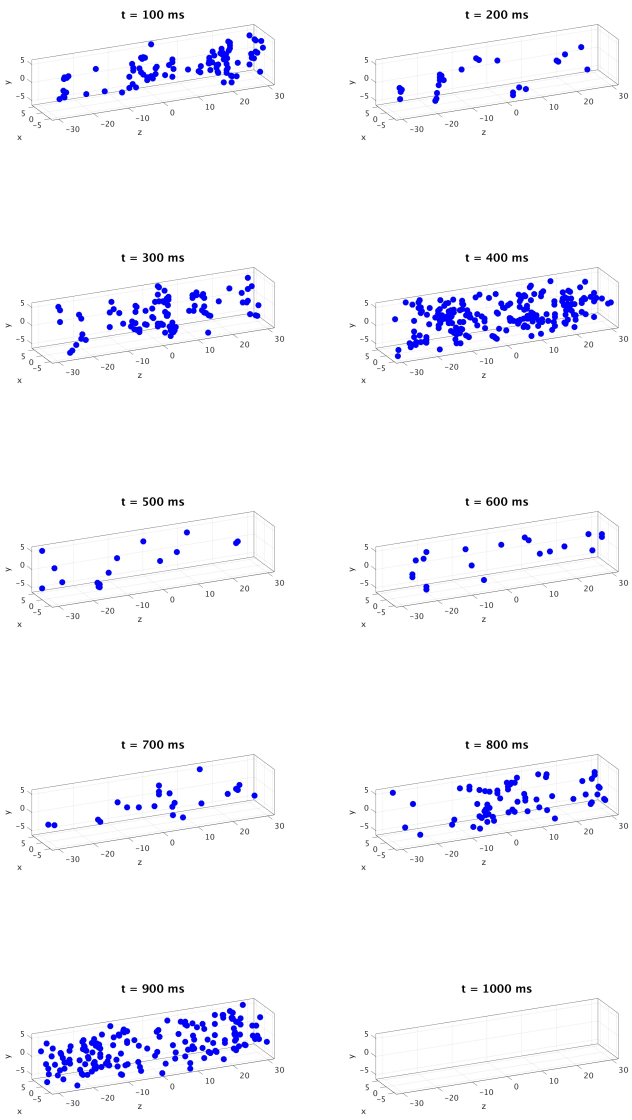

Figure 5.14: CRU open plots for wave with $\omega = 30$.

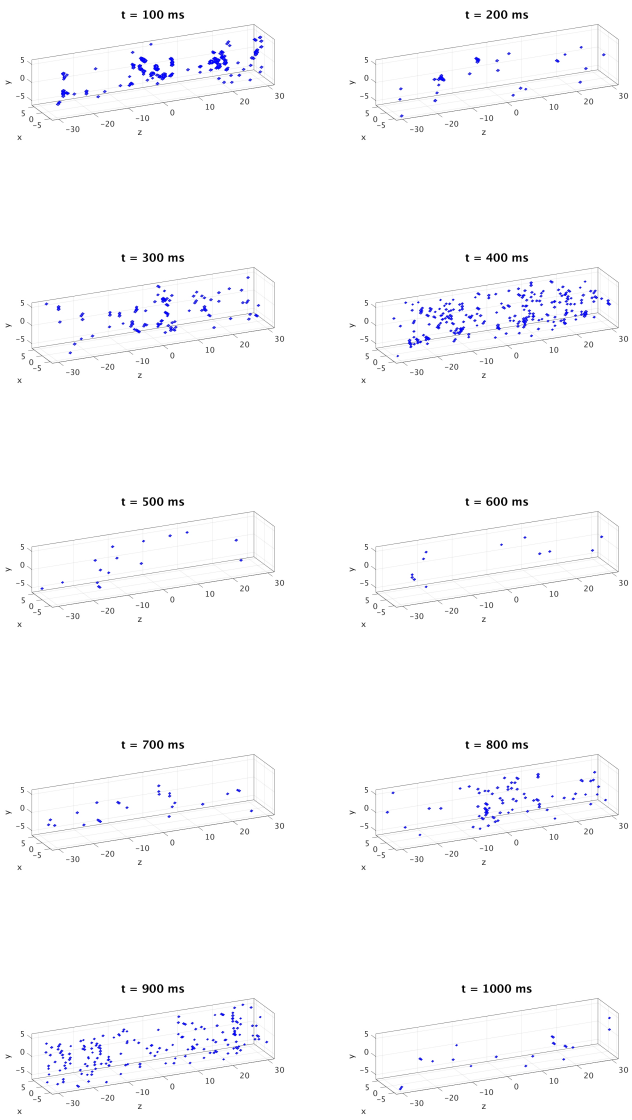

Figure 5.15: ISO open plots for wave with $\omega = 30$.

5.2.3 Spark

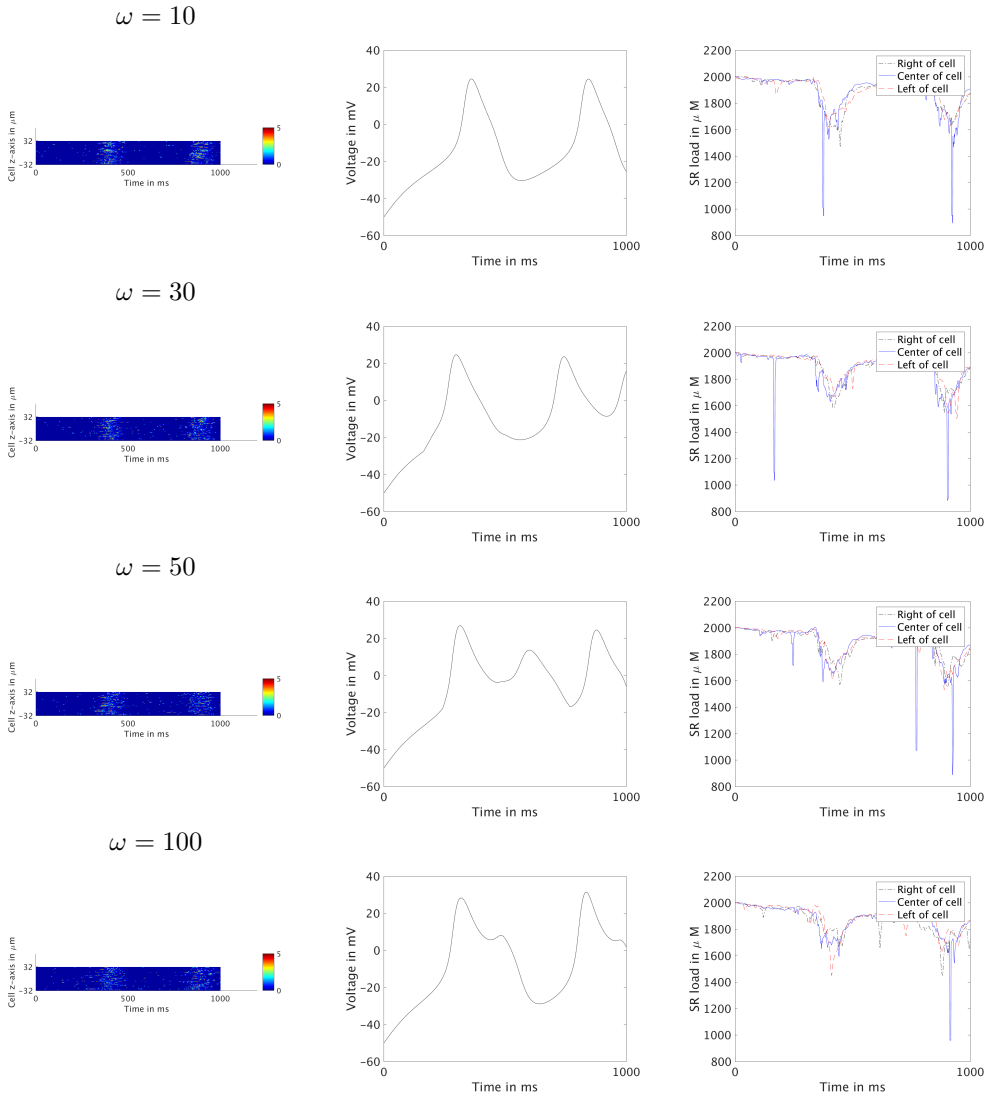

Figure 5.16: Line Scans, Voltage Plots, and SR Plots for a spark for $\omega = 10, 30, 50$ and , 100.

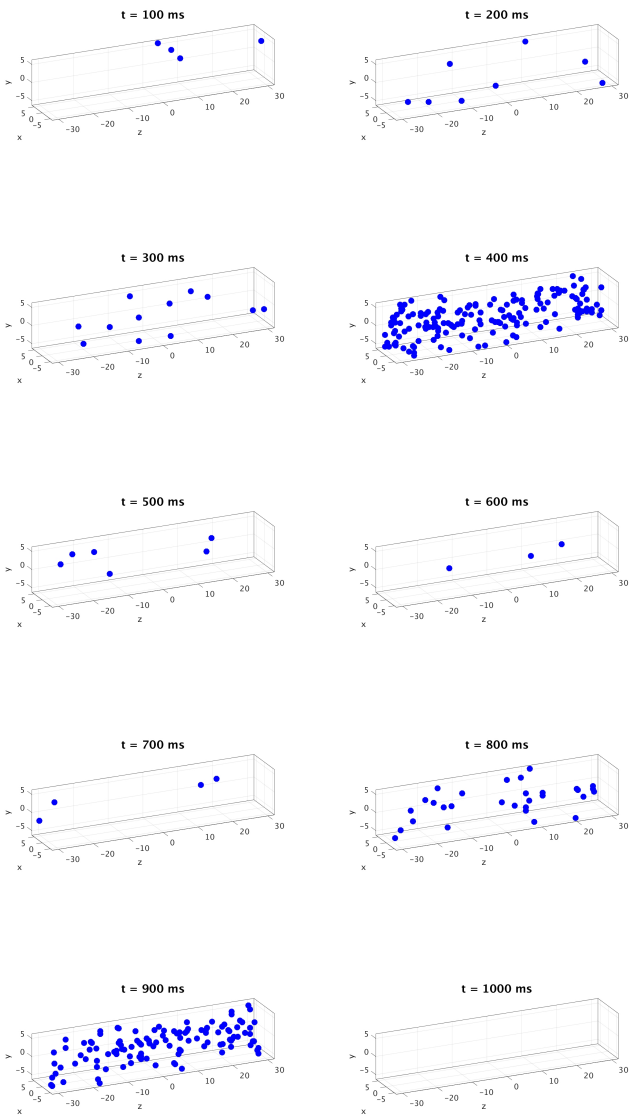

Figure 5.17: CRU open plots for spark with $\omega = 30$.

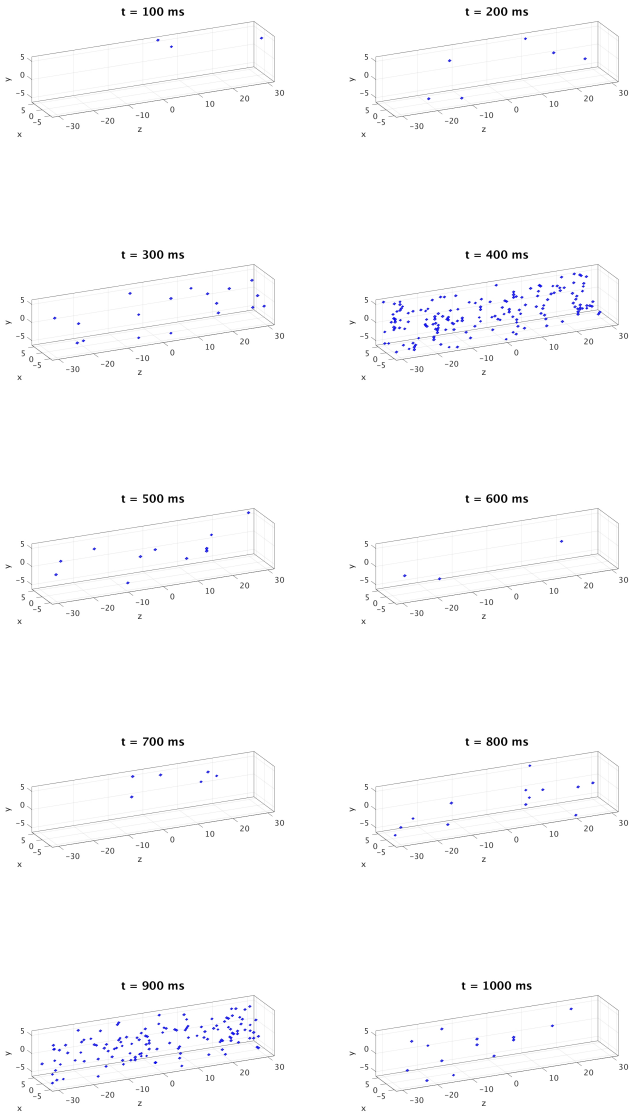

Figure 5.18: ISO open plots for spark with $\omega = 30$.

6 Conclusions

Our extended model completes the links between the electrical, calcium, and mechanical systems; the simulations presented here study coupling between the electrical and calcium systems.

We linked the calcium and mechanical systems via feedback and feed-forward terms for the contractile dynamics model, using the proportion of actin-myosin cross-bridges which are actively linked and therefore generating contractile force at any given time. We introduced a new cytosol species to describe these actin-myosin cross-bridges and introduced a corresponding third cytosol reaction term. We also modified the reaction equation for troponin to more accurately describe the decreased calcium-troponin disassociation rate resulting from the protein's change in shape.

We introduced a calcium dependency into the voltage PDE, controlled by a scaling factor of feedback strength ω. The calcium efflux term $(J_{m_{pump}} - J_{m_{leak}})$ represents the only coupling between cytosol calcium levels and voltage in the full set of PDEs, which can be switched on or off by making the feedback strength parameter ω a positive value or zeroing it out to sever the connection from the calcium dynamic to the electrical dynamic. Our parameter study indicated that as ω increased, the effect on voltage increased correspondingly, as is physiologically realistic. Our initial guesses for ω were too low to produce notably altered results; feedback strengths below a value of 10 did not have dramatic effects on the voltage. However, as we continued to scale ω up, we began to see a stronger and stronger influence of the current generated by calcium efflux through the membrane upon the electrical potential of the membrane itself. The formerly steady and unaffected periodicity of the voltage over time first sped up, then deteriorated altogether, as we continued to increase the value.

Future directions of this research include implementation in C of the third cytosol buffer species in our model, the actin-myosin cross-bridges: while we have established the grounds for the behavior of this species mathematically, it has not yet been examined programatically. Other avenues of investigation include further parameter studies of ω and κ, as our introduction of ω has enabled a more direct representation of the relationship between cytosol calcium concentration and membrane potential.

Acknowledgments

These results were obtained as part of the REU Site: Interdisciplinary Program in High Performance Computing (hpcreu.umbc.edu) in the Department of Mathematics and Statistics at the University of Maryland, Baltimore County (UMBC), in Summer 2016. This program is funded by the National Science Foundation (NSF), the National Security Agency (NSA), and the Department of Defense (DOD), with additional support from UMBC, the Department of Mathematics and Statistics, the Center for Interdisciplinary Research and Consulting (CIRC), and the UMBC High Performance Computing Facility (HPCF). HPCF is supported by the U.S. National Science Foundation through the MRI program (grant nos. CNS–0821258 and CNS–1228778) and the SCREMS program (grant no. DMS–0821311), with additional substantial support from UMBC. Co-author Uchenna Osia was supported in part by the UMBC National Security Agency (NSA) Scholars Program through a contract with the NSA. Graduate assistant Jonathan Graf was supported by UMBC.

References

[1] Amanda M. Alexander, Erin K. DeNardo, Eric Frazier III, Michael McCauley, Nicholas Rojina, Zana Coulibaly, Bradford E. Peercy, and Leighton T. Izu. Spontaneous calcium release in cardiac myocytes: Store overload and electrical dynamics. *Spora: A Journal of Biomathematics*, 1(1), 2015.

[2] Tamas Banyasz, Balazs Horvath, Zhong Jian, Leighton T Izu, and Ye Chen-Izu. Profile of l-type ca 2+ current and na+/ca 2+ exchange current during cardiac action potential in ventricular myocytes. *Heart Rhythm*, 9(1):134–142, 2012.

[3] Matthias K. Gobbert. Long-time simulations on high resolution meshes to model calcium waves in a heart cell. *SIAM J. Sci. Comput.*, 30(6):2922–2947, 2008.

[4] Alexander L. Hanhart, Matthias K. Gobbert, and Leighton T. Izu. A memory-efficient finite element method for systems of reaction-diffusion equations with non-smooth forcing. *J. Comput. Appl. Math.*, 169(2):431–458, 2004.

[5] Leighton T. Izu, Shawn A. Means, John N. Shadid, Ye Chen-Izu, and C. William Balke. Interplay of ryanodine receptor distribution and calcium dynamics. *Biophys. J.*, 91:95–112, 2006.

[6] Leighton T. Izu, W. Gil Wier, and C. William Balke. Evolution of cardiac calcium waves from stochastic calcium sparks. *Biophys. J.*, 80:103–120, 2001.

[7] Catherine Morris and Harold Lecar. Voltage oscillations in the barnacle giant muscle fiber. *Biophysical journal*, 35(1):193, 1981.